ELSEVIER

Journal of Photochemistry and Photobiology A: Chemistry 95 (1996) 7–20

Journal of PHOTOCHEMISTRY AND PHOTOBIOLOGY A: CHEMISTRY

Nonradiative twisted intramolecular charge transfer state in polar stilbenes: photophysical study of 4-perfluorooctylsulfonyl-4′-*N*,*N*-dimethylamino stilbene and two bridged derivatives *

H. Le Breton [a], B. Bennetau [a], J.-F. Létard [b,1], R. Lapouyade [b,1], W. Rettig [c]

[a] *Laboratoire de Chimie Organique et Organométallique, Université Bordeaux 1, Unité de Recherche associé au CNRS 35, 351 cours de la Libération, 33405 Talence, France*

[b] *Laboratoire de Photophysique et Photochimie Moléculaire, Université Bordeaux 1, Unité de Recherche associée au CNRS 348, 351 cours de la Libération, 33405 Talence, France*

[c] *Institute for Physical and Theoretical Chemistry, Humboldt University Berlin, Bunsenstrasse 1, D-10117 Berlin, Germany*

Abstract

Photoinduced intramolecular electron transfer has been studied in 4-perfluorooctylsulfonyl-4′-*N*,*N*-dimethylamino stilbene (PFSDS) and its bridged derivatives (PFSDS-O23 [2] and PFSDS-N34 [2]) where the central double bond is rigidized by a heteroatom. Excited-state dipole moments have been obtained from the solvatochromic behavior of the fluorescence. The decrease in the fluorescence quantum yields and the shortening of the fluorescence lifetimes in polar solvents have been analyzed. Semiempirical calculations suggest that the twisted intramolecular charge transfer (TICT) states A_4^* (S_7) for PFSDS, A_4^* (S_7) for PFSDS-O23 and A_2^* (S_{18}) for PFSDS-N34 are sufficiently low lying to become the lowest excited states in polar solvents because of their high dipole moments. The photophysical results suggest non-radiative properties for most of the TICT states and the accessibility of a higher energy emissive TICT state for PFSDS only.

Keywords: Polar stilbenes; Nonradiative TICT states; Stilbene

1. Introduction

Aromatic systems with strong electron donor and acceptor substituent groups have been the subject of continuous theoretical and experimental interest. The donor–acceptor diphenyl polyenes have been proposed for potential soliton switching devices [2] and show promising applications in non-linear optics (NLO) [3]. The donor–acceptor stilbenes are the simplest unit of this series of molecules and have favorable properties for second-order non-linear optics [4]. However, while nitro and polycyanovinyl groups have been widely studied as acceptor groups, the sulfonyl group has not received much attention despite its strong acceptor properties [5]: for example, its σ_p and σ^- values are +0.72 and +1.05 respectively, while for the nitro group these values are +0.79 and +1.24 respectively. Nevertheless, recent studies have shown that strong inductive acceptor groups, such as the fluoromethyl carbonyl and perfluoroalkyl sulfonyl groups, afford favorable trade-off between quadratic optical non-linearity and optical transparency and then suggest promising applications in the frequency conversion of short-wavelength diode lasers [6–8]. Recently, we have presented a structural characterization of Langmuir–Blodgett (LB) films of three new polyphilic polar stilbenes: the 4-*N*,*N*-dimethylamino-4′-heptadecafluorooctylsulfonyl stilbene (PFSDS) [9] and some analogues, 2-(4′-*N*,*N*-dimethylanilino)-6-heptadecafluorooctylsulfonyl indole (PFSDS-N34) [9] and 2-(4′-heptafluorooctylsulfonylphenyl)-6-*N*,*N*-dimethylamino benzofuran (PFSDS-O23) [9,10] (Fig. 1), in which the central double bond is incorporated in a five-membered ring containing one heteroatom such as nitrogen and oxygen atoms. The second-order molecular hyperpolarizability of these molecules in LB films is relatively high ($\beta \approx 2 \times 10^{-28}$ esu) and, in particular when the double bond is bridged with

* In honour of Professor Stefan Paszyc.

[1] Present address: Laboratoire des Sciences Moléculaires, Institut de Chimie de la Matière Condensée de Bordeaux, Château de Brivazac, avenue du Dr. A. Schweitzer, 33608 Pessac Cédex, France.

[2] The numbers 2,3 and 3,4 indicate the position of the five-membered ring relative to the NMe_2 group, as in the nomenclature proposed in [1] and presented in Fig. 1. The symbols *O* and *N* represent respectively the oxygen and the nitrogen heteroatoms incorporated into the five-membered ring, which bridges the central double bond of the stilbene chromophore.

SSDI 1010-6030(95)04231-8

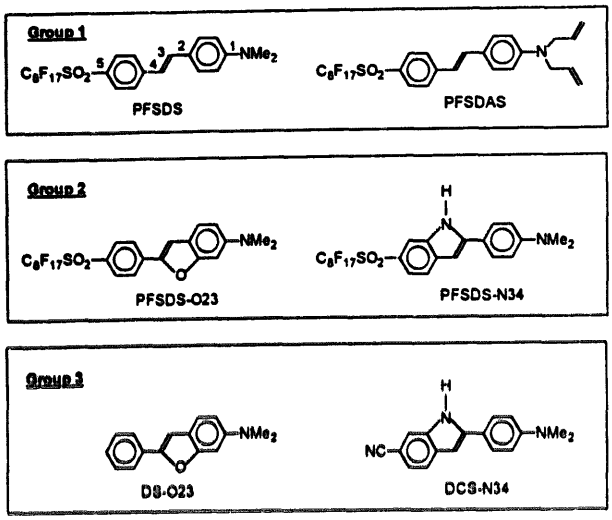

Fig. 1. Molecular structure of the investigated compounds.

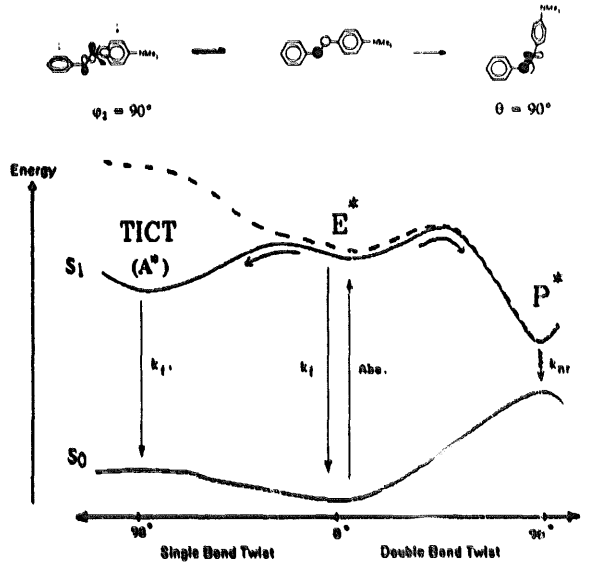

Scheme 1. Energy scheme proposed for the solvent effect on the photophysical behavior of donor–acceptor stilbenes [1,14–18] (DS derivatives). In the gas phase (- - -) the planar conformation (E* state, polar, emissive) is the lowest state, whereas in polar solvents the perpendicular single-bond conformation (TICT state, highly polar, emissive) has a lower energy because of the high dipole moment and competes with the channel E* → P* (twisted double bond, weakly polar, non-emissive). The TICT fluorescence for DS corresponds to a perpendicular single bond conformation where the donor (dimethylaniline) and the acceptor groups (styrene) are orbitally decoupled ($\varphi_2 = 90°$), with strong orbital coefficients at the linking C–C atoms [18].

a heteroatom (O or N), they present an increased photostability under the conditions for second-harmonic generation [9].

In the present work, we report the synthesis and the study of the photophysical properties of these three new donor–acceptor stilbenes. The effects of solvent polarity on the spectral position of fluorescence, fluorescence quantum yields and lifetimes of these molecules were examined and quantum-chemical calculations of ground and excited states were carried out in order to understand the peculiar behavior of PFSDS-N34 and PFSDS-O23, which present an anomalous decrease in the fluorescence quantum yields in polar solvents.

Some of the questions which we try to answer are as follows.

(i) Is there an involvement of low-lying non-emissive twisted internal charge transfer (TICT [11–13]) states by rotation of bonds 2 or 4? In this case, why are these TICT states non-emissive for PFSDS derivatives and emissive for 4-*N*,*N*-dimethylamino-4′-cyano stilbene (DCS) [14–16] and 4-*N*,*N*-dimethylamino stilbene (DS) [1,17,18] (Scheme 1)?

(ii) Is there a further non-radiative channel in PFSDS derivatives involving the twisting of the acceptor group ($-SO_2C_8F_{17}$), as recently proposed to explain the decrease in the fluorescence quantum yield of 4-*N*,*N*-dimethylamino-4′-nitro stilbene (DNS) in polar solvents [19], where a rotation of the $-NO_2$ group has been proposed?

2. Methods

2.1. Experimental details

2-(4′-heptafluorooctylsulfonylphenyl)-6-*N*,*N*-dimethylaminobenzofuran (PFSDS-O23) was synthesized as previously described [10]. The other stilbenes (DS-O23, DCS-N34, PFSDS and PFSDS-N34) were obtained by the route outlined in Scheme 2. All the compounds were purified by column chromatography on silica gel followed by crystallization.

Solvents were of spectroscopic quality (SDS or Merck). The absorption spectra and the fluorescence spectra were

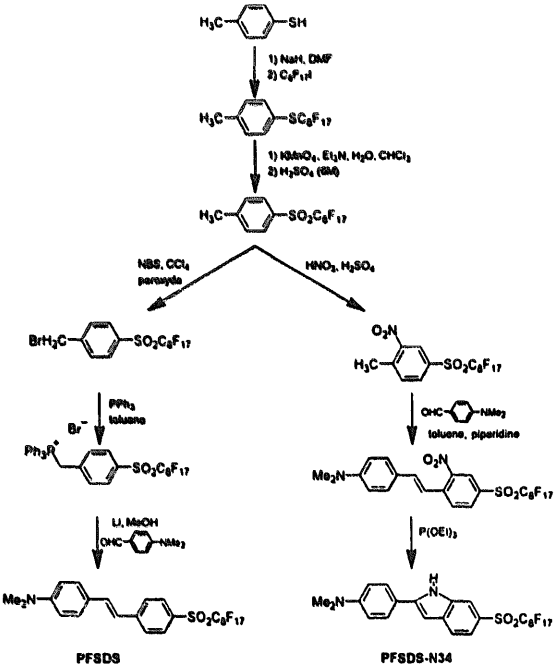

Scheme 2. Route followed for the synthesis of PFSDS and PFSDS-N34.

determined on a Hitachi U-3300 and on a Hitachi F-4500 spectrometer respectively. The standard for the fluorescence quantum yield determinations was quinine bisulfate in 1 N H_2SO_4 ($\phi_f = 0.55$), and after solvent refractive index correction the experimental errors are judged ± 10%. Fluorescence decays of aerated solutions were measured using a single-photon-counting set-up described in detail elsewhere [20] and synchrotron radiation from BESSY as the excitation source. The limit of the detection is 100 ps.

2.1.1. 4-heptadecafluorooctyl-2-nitrotoluene

A solution of *p*-heptadecafluorooctylsulfonyl toluene (5 g, 8.7 mmol) and concentrated H_2SO_4 (8.5 ml) were stirred. Then fuming HNO_3 (2.19 g, 34.8 mmol) was added dropwise. After the addition, the mixture was heated to 150 °C for 30 min. The cooled solution was poured onto 100 g of ice, extracted with diethyl ether, washed with a solution of NaOH (15%), dried over $MgSO_4$ and evaporated to dryness to give the desired product (yield, 5.2 g, 8.4 mmol (96%)). ^{1}H NMR ($CDCl_3$, 250 MHz): δ 2.7 (s, 3H, $-CH_3$), 7.7 (d, 1H, $-H_6$, $J = 8.2$ Hz), 8.1 (dd, 1H, $-H_2$, $J = 8.1$ Hz, $J = 1.5$ Hz), 8.5 (d, 1H, $-H_3$, $J = 1.5$ Hz) ppm. ^{13}C NMR ($CDCl_3$, 250 MHz): δ 20.8 ($-CH_3$), 127.3, 134.2, 134.8 ($-C_{Ar}$–H), 131.2, 143.2, 150 ($-C_q$) ppm.

2.1.2. 4-heptadecafluorooctylsulfonyl-2-nitro-4′-N,N-dimethylaminostilbene

A solution of 4-heptadecafluorooctylsulfonyl-2-nitro toluene (3 g, 4.85 mmol) and 4-*N*,*N*-dimethylamino benzaldehyde (0.77 g, 5.2 mmol) in toluene (15 ml) was stirred. Then some drops of piperidine were added and the mixture was heated to 150 °C for 30 min. After cooling, the desired product was filtered and recrystallized in methyl alcohol (yield, 3 g, 3.99 mmol (82%)). ^{13}C NMR ($CDCl_3$, 250 MHz): δ 40.1 ($-N(CH_3)_2$), 112.0, 114.8, 128, 128.4, 129.7, 133.4, 140.4, ($-C_{Ar}$H), 123.3, 128.6, 141.6, 147, 151.8 (C_q) ppm. Anal. Found: C, 38.41; H, 2.01; N, 3.73; S, 4.27; F, 43.04. $C_{24}H_{15}F_{17}N_2O_4S$ calc.: C, 38.18; H, 2.06; N, 3.89; S, 4.95; F, 43.37.

2.1.3. PFSDS-N34

A solution of 4-heptadecafluorooctylsulfonyl-2-nitro-4′-*N*,*N*-dimethylamino stilbene (2.5 g, 3.33 mmol) in $P(OEt)_3$ (17 ml) was stirred and refluxed during one night. The final product was purified by chromatography on silica gel (CH_2Cl_2:pentane: 1.1 v/v) to give a yellow powder which was recrystallized in petroleum ether:$CHCl_3$ (1:1, v/v) (yield, 0.4 g, 0.56 mmol (20%)). ^{1}H NMR ($CDCl_3$, 250 MHz) δ: 3 (s, 6H, $-N(CH_3)_2$, 6.84, 6.88, 7.78, 7.82 ($4H_{ar}$, H_2, H_3, H_5, H_6, system AA′BB′), 6.97 (s, $1H_{ar}$, H_8), 7.6 (d, $1H_{ar}$, H_{13}, $J_{H^{13}-H^{14}} = 8$ Hz), 7.8 (d, $1H_{ar}$, H_{14}, $J_{H^{14}-H^{13}} = 8$ Hz), 8.1 (s, 1H, N–H) ppm. ^{13}C NMR ($CDCl_3$, 250 MHz): δ 40.2 ($-N(CH_3)$, 98.5, 113.2, 115.5, 121, 122, 127.9 (C_{ar}–H), 119, 121.5, 136.7, 137.3, 147.5, 152.2 (C_q) ppm. Anal. Found: C, 40.12; H, 2.10; N, 3.90; F, 44.96 (45.11). $C_{24}H_{15}F_{17}N_2O_2S$ calc.: C, 40.51; H, 2.18; N, 3.98; F, 45.11.

2.1.4. p-heptadecafluorooctylsulfonyl benzyltriphenyl phosphonium

A stirred solution of *p*-heptadecafluorooctylsulfonylbenzyl bromide (1 g, 1.53 mmol), triphenyl phosphine (0.81 g, 3.1 mmol) and dry toluene (50 ml) was refluxed for 2 h. After cooling, the product was filtered (yield, 0.85 g, 0.93 mmol (61%)). ^{1}H NMR ($CDCl_3$, 250 MHz): δ 6.1 (d, 2H, $-CH_2$–Ph, $J_{H-P^+} = 16$ Hz), 7.46–7.77 (m, 19H, H_{ar}) ppm.

2.1.5. PFSDS

p-heptadecafluorooctylsulfonyl benzyl triphenyl phosphonium (0.85 g, 0.93 mmol) and *p*-*N*,*N*-dimethylamino benzaldehyde (0.138 g, 0.93 mmol) were added to a stirred solution of lithium (16 mg, 2.32 mmol) and methyl alcohol (15 ml). The mixture was stirred under nitrogen at room temperature during one night. After the addition of water (50 ml), the product was extracted with $CHCl_3$ (2×15 ml), washed with water and dried over $MgSO_4$. The final product was chromatographed on silica gel (pentane:$CHCl_3$, (7:3 v/v) and recrystallized from CH_2Cl_2:petroleum ether (1:1, v/v) to give a yellow powder of PFSDS (E) (yield, 150 mg, 0.21 mmol (25%)). Melting point, 191 °C. ^{1}H NMR ($CDCl_3$, 250 MHz): δ 3 (s, 6H, $-N(CH_3)_2$), 6.7, 6.74, 7.44, 7.48, ($4H_{ar}$, system AA′BB′), 6.89, 6.96, 7.24, 7.31 ($H_{olefinic}$, system AB, $J_{trans} = 16$ Hz), 7.65, 7.69, 7.91, 7.95 ($4H_{ar}$, system AA′BB′). Mass spectroscopy: 704.9 (93), $M^{+\cdot}$ molecular peak; 222 (100) ($-SO_2C_8F_{17}$).

2.2. Calculations

The AMPAC 5.0 package [21] has been used for the calculation, within the AM1 framework [22], of the ground-state energies E_g for planar and perpendicular conformations of 4-*N*,*N*-dimethylamino-4′-trifluoromethylsulfonyl stilbene and of the 4′-trifluoromethylsulfonyl analogues of PFSDS-O23 and PFSDS-N34. The energy gaps ΔE between ground and excited states were calculated within the CNDO/S formalism of Del Bene and Jaffé [23] using QCPE Program No. 333 modified for large molecules and the calculation of excited-state dipole moments. The cut-off energy for configuration interaction was 15 eV (usually 50 singly excited configuration). Quantum-chemical calculations of DS-O23 and DCS-N34 were not performed.

The geometry of the benzene rings was idealized, i.e. $d_{C-C} = 1.40$ Å and $d_{C-H} = 1.083$ Å with an angle of 120°. The ethylenic bond length was $d_{C=C} = 1.33$ Å and the bond lengths connecting to the benzene rings $d_{C-C} = 1.45$ Å with an angle of 128° [24]. The bond lengths of the dimethylamino group were defined as $d_{C_{ar}-N} = 1.37$ Å and $d_{N-CH_3} = 1.46$ Å [25]. The geometry of the trifluoromethyl sulfonyl group was taken as follows: $d_{C_{ar}-S} = 1.76$ Å, $d_{C-S} = 1.776$ Å, $d_{S-O} = 1.437$ Å, $d_{C-F} = 1.32$ Å [26] and angles $\langle C_{ar}-S-C\rangle = 102°$ [26], $\langle O-S-O\rangle = 109°$ [27]. The structural parameters of the benzofuran, the indole and the position of the $-CF_3$ group relative to the phenyl plane were determined by minimizing the total energy. All structural parameters were kept constant

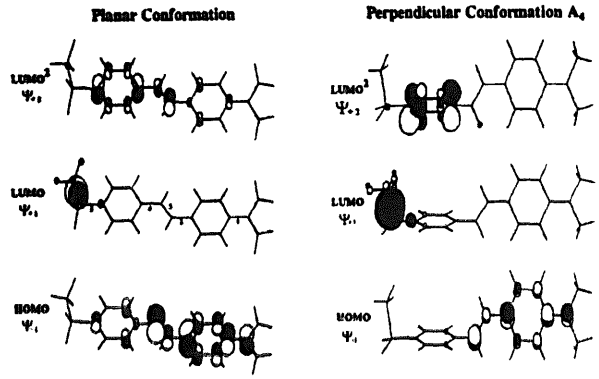

Fig. 2. 4-*N,N*-dimethylamino-4'-trifluoromethylsulfonyl stilbene: orbital representations for the (a) planar and (b) perpendicular conformation (A_4) for the highest occupied molecular orbital (HOMO) Ψ_{-1}, the lowest unoccupied molecular orbital (LUMO) Ψ_{+1} and the second-lowest unoccupied molecular orbital (LUMO^2) Ψ_{+2}. The molecular orbitals were drawn by the program MO-PLOT [28] in a recently updated version by Bally *et al.* [29]. (a) For the planar conformation, the transition $\chi_{-1}{}^{+2}$ represents the preponderant weight (80%) of the S_3 state, which has the highest oscillator strength ($f = 0.6$) and a dipole moment of 32 D. The $\chi_{-1}{}^{+1}$ transition, which represents the main part (41%) of the E* (S_4) state, has a strong charge transfer character involving near one-electron transfer from the DS ($\Delta q = +0.89$) to the $-SO_2$ group ($\Delta q = -0.89$) and then a high excited-state dipole moment ($\mu_e = 45$ D). It can be seen in the S_4 state that the HOMO and LUMO possess large orbital coefficients at the C and S atoms which links the donor and acceptor ($-SO_2R$) parts. (b) In the perpendicular conformation A_4, the transition $\chi_{-1}{}^{+2}$ (67% of the TICT A_4* (S_5)) involves an electron transfer from the *p-N,N*-dimethylamino styrene ($\Delta q = +0.96$) to the trifluoromethylsulfonylphenyl group ($\Delta q = -0.96$), with large atomic orbital coefficients at bond 4 around which the donor and the acceptor groups decouple. The state A_4* (S_7) (main transition $\chi_{-1}{}^{+1}$, 72%), which is the lowest state in polar solvent (Fig. 3), has a strong charge transfer character involving, as TICT A_4* (S_5), an electron transfer from the *p-N,N*-dimethylamino styrene ($\Delta q = +0.98$) to the trifluoromethylsulfonylphenyl group ($\Delta q = -0.98$), but now centred on the SO_2R group. Then, we can see the $\chi_{-1}{}^{+1}$ transition small orbital coefficients at the atoms which link the donor and acceptor parts.

during internal rotation of the different single and/or double bonds.

Dihedral angles between the π moieties linked by the relevant bond were assumed to be zero for the planar conformations, with the plane defined by CF_3–SO_2–C_{ar} perpendicular to the phenyl ring. For the twisted conformations, a 90° rotation was realized from the planar conformation. For a short-hand notation we shall call the conformer with the perpendicular twisted single bond A_i (with i indicating the bond twisted (Fig. 2)) and the lowest TICT excited state A_i*, as proposed recently for the study of DS [18].

The solvation energy E_g^{solv} of the ground state and the solvation energy E_e^{solv} of the excited state are calculated according to the following equation [30,31], using the solvation model derived from the Onsager theory [32]:

$$E_i^{solv} = \frac{\mu_i^2}{4\pi\varepsilon_0\rho^3} f(\epsilon) \quad (1)$$

with

$$f(\epsilon) = \frac{\epsilon - 1}{2\epsilon + 1} \quad (1a)$$

and

$$\rho = \left(\frac{3M}{4\pi d}\right)^{1/3} \quad (1b)$$

The cavity radius ρ is derived from the molecular volume, as calculated (Eq. (1b)) from the molecular weight M and the density d of 1.252 g cm^{-3} for diphenylsulfone [26]. Eq. (1), where μ_i denotes the dipole moment of the corresponding states i, applies when the solvent is fully equilibrated around the dipole μ_i. The energies of the solvated ground and excited states (E_g^s and E_e^s respectively), derived from the following equations, assumes the planar solvated ground state as the reference energy [18]:

$$E_g^s = E_g - E_g^{solv} \quad (2)$$

$$E_e^s = E_g + \Delta E - E_e^{solv} + E_g^{solv} \quad (3)$$

3. Results

3.1. Semiempirical calculations

Tables 1, 2 and 3 give the values of the ground-state energy and dipole moment of PFSDS, PFSDS-O23 and PFSDS-N34 for the planar conformation and also for the perpendicular conformations around the single bonds (bonds 1, 2, 4, 5) and the double bond (bond 3) when these bonds are not constrained in a five-membered ring (Fig. 1). For each conformation, the excited state energy E_e, the oscillator strength f and the dipole moment μ_e for the singlet excited states of these three derivatives are presented in the tables, too.

For the planar conformation of the three derivatives, the first electronic transition has a small oscillator strength (0.04–0.05) and the corresponding excited state a dipole moment of around 16 D, except for PFSDS-N34, which is more polar (23.9 D). The state S_3 of PFSDS derivatives is the first which possesses a high oscillator strength ($0.5 \leqslant f \leqslant 0.6$) and a relatively high dipole moment (30–32 D). However, the state S_4, for the three derivatives, is characterized by the highest dipole moments: 44.7 D (PFSDS), 45.6 D (PFSDS-O23) and 36.2 D (PFSDS-N34). Note that the relative magnitude of the dipole moment of E^* (S_4) is the lowest for PFSDS-N34.

Only for PFSDS can the double bond reach the perpendicular conformation (Scheme 1). In agreement with the current theoretical model of olefin isomerization [33–35], the potential energy curves of ground state and S_1 state exhibit a very small energy gap for this geometry. The results of calculations on PFSDS in the perpendicular double-bond conformation indicate a lower dipole moment for the first excited state P* ($\mu_e = 11.2$ D) than for the ground state P_0 ($\mu_g = 15.2$ D). Such observation is consistent with the biradicaloid model,

Table 1
Energy E_g (eV) and dipole moment μ_g (D) of the ground state estimated by AMPAC 5.0 for the planar and perpendicular twisted conformations A_i of PFSDS (see Fig. 2 for definition of indices). The energy E_e (eV), oscillator strength f and dipole moments μ_e (D) of PFSDS in the excited states are calculated within the CNDO/S framework. The energy of the solvated excited states is also estimated in *n*-hexane (f=0.185), diethyl ether (Et_2O) (f=0.345), tetrahydrofuran (f=0.407) and acetonitrile (CH_3CN (f=0.480)) according to Eqs. (1)–(3)

		Planar	Twisted A_1	Twisted A_2	Twisted A_3	Twisted A_4	Twisted A_5
State S_0	E_g	0	0.34	0.13	2.40	0.07	0.33
	μ_g	11.8	9.7	10.9	15.2	11.1	11.6
State S_1	E_e	3.10	3.43	3.23	2.68	3.17	3.44
	f	0.04	0.04	0.03	7.10^{-5}	0.02	0.05
	μ_e	15.7	11.5	14.2	11.2	12.2	12.9
State S_2	E_e	3.33	3.67	3.46	5.05	3.40	3.65
	f	0.0000	0.0000	0.0000	0.003	0.0000	1.10^{-5}
	μ_e	10.7	9.8	11.2	42.6	11.0	29.8
State S_3	E_e	3.79	4.21	4.22	5.55	4.10	4.13
	f	0.62	0.18	0.001	0.06	0.002	0.63
	μ_e	32.5	41.7	11.4	21.7	21.1	28.1
State S_4	E_e	3.98	4.28	4.37	5.58	4.38	4.22
	f	0.012	0.45	7.10^{-4}	6.10^{-4}	0.01	6.10^{-4}
	μ_e	44.7	26.1	31.8	13.1	14.1	34.6
State S_5	E_e	4.09	4.73	4.56	5.65	4.52	4.51
	f	0.001	0.001	0.017	0.02	8.10^{-3}	6.10^{-4}
	μ_e	10.9	15.4	16.7	29.1	46.1	28.2
State S_n	E_e		5.54 (S_{12})	4.74 (S_9)		4.71 (S_7)	
	f		0.0000	4.10^{-3}		2.10^{-3}	
	μ_e		44.7	45.4		53.2	

Conformations	States	Gas phase	n-hexane	Et_2O	THF	CH_3CN
Planar	S_1	3.10	3.05	3.00	2.98	2.96
	S_2	3.33	3.34	3.35	3.36	3.36
	S_3	3.79	3.32	2.92	2.77	2.58
	S_4	3.98	3.04	2.22	1.90	1.53
Twisted A_1	S_{12}	5.54	4.57	3.74	3.41	3.03
Twisted A_2	S_9	4.74	3.75	2.90	2.57	2.18
Twisted A_4	S_5	4.52	3.50	2.62	2.28	1.88
	S_7	4.71	3.34	2.15	1.69	1.14

which predicts a state inversion for the double-bond twisted species as one goes from symmetric stilbene (where $\mu_g^{Po} = 0$ D and $\mu_e^{P*} = 8$ D) to donor–acceptor stilbenes [36].

Twisting about the different single bonds for PFSDS can lead in principle to TICT states A_1*, A_2*, A_4* and A_5* where different donor and acceptor moieties decouple. A TICT state is identified by a high dipole moment and a very low oscillator strength. CNDO/S calculations indicate for PFSDS the presence of TICT states only for twisting of bonds 1, 2 and 4 (Table 1). In the gas phase, the TICT state A_4* (S_5) is the lowest in energy, followed by A_4* (S_7), A_2* (S_9) and A_1* (S_{12}). Such results are in accordance with our previous CNDO/S calculations on various donor–acceptor stilbenes, which showed a preference of the decoupling bond towards the acceptor site when its electron acceptor strength was increased [19]. For twisted bond 5, where the SO_2–CF_3 bond is in the plane of the phenyl ring, calculations do not detect any TICT state in the 25 first excited states, which correspond to an energy gap ΔE of 6.50 eV.

Taking into account that bond 2 is maintained planar in PFSDS-O23 (Table 2) and bond 4 for PFSDS-N34 (Table 3) the succession of A* states are the following in the gas phase: for PFSDS-O23, A_4* (S_3) is the lowest in energy followed by A_4* (S_7), A_5* (S_8) and A_1* (S_{28}); for PFSDS-N34, A_2* (S_{10}) is the lowest TICT state followed by A_2* (S_{18}) and, at very much higher energy, A_5* (S_{27}) and A_1* (S_{29}).

If now solvation is taken into account, using Eqs. (1)–(3), for the planar conformation (E) of the three derivatives, because of its high dipole moment, the state E* (S_4) becomes the lowest excited state already in *n*-hexane or diethyl ether (Tables 1–3 and Fig. 3). Although these equations lead to energies of solvated states which are discussed below, their approximate character (owing to the uncertainties in the cal-

Table 2
Same as Table 1 but for PFSDS-O23

		Planar	Twisted A_1	Twisted A_4	Twisted A_5
State S_0	E_g	0	0.35	0.16	0.31
	μ_g	11.4	9.4	10.4	11.1
State S_1	E_e	3.10	3.45	3.27	3.42
	f	0.05	0.04	0.024	0.06
	μ_e	16.1	10.8	11.3	13.2
State S_2	E_e	3.34	3.68	3.49	3.63
	f	0.0000	0.0000	0.0000	1.10^{-5}
	μ_e	10.1	9.1	11.6	27.8
State S_3	E_e	3.54	4.02	4.22	3.86
	f	0.51	0.51	6.10^{-3}	0.51
	μ_e	31.2	29.1	41.7	27.4
State S_4	E_e	3.92	4.27	4.29	4.18
	f	0.003	0.006	0.05	5.10^{-4}
	μ_e	45.6	40.7	14.8	38.3
State S_5	E_e	4.09	4.54	4.31	4.44
	f	0.001	0.009	0.002	0.004
	μ_e	10.3	18.4	18.2	16.8
State S_8	E_e		7.02 (S_{28})	4.50 (S_7)	4.84 (S_8)
	f		0.0000	1.10^{-3}	8.10^{-3}
	μ_e		63.6	52.6	44.3

Conformations	States	Gas phase	n-hexane	Et_2O	THF	CH_3CN
Planar	S_1	3.10	3.03	2.98	2.96	2.97
	S_2	3.34	3.35	3.37	3.37	3.37
	S_3	3.54	3.11	2.74	2.60	2.66
	S_4	3.92	2.93	2.07	1.74	1.35
Twisted A_1	S_{28}	7.02	5.01	3.27	2.60	2.30
Twisted A_4	S_3	4.22	3.39	2.68	2.40	2.52
	S_7	4.50	3.15	1.98	1.53	1.00
Twisted A_5	S_8	4.84	3.91	3.10	2.79	2.42

culated dipole moments and in the assumed Onsager cavity radius) should be kept in mind. The calculations are, however, valid to assess which of the high-lying states can become photochemically relevant owing to solvation and are used in this sense in the discussion.

For PFSDS (Table 1), in acetonitrile, two TICT states have energies close to that of $E^*(S_4)$ (1.53 eV): TICT states A_4^* (S_5) (1.88 eV) and A_4^* (S_7) (lowered to 1.14 eV). The TICT state A_4^* (S_7) corresponds to a similar transition as the S_4 state of the planar conformation (Fig. 2), that is to promotion of an electron from the HOMO Ψ_{-1} to the LUMO Ψ_{+1} denoted χ_{-1}^{+1}, where χ_i^j signifies a one-electron configuration with excitation from orbital Ψ_i to orbital Ψ_j. However, the TICT state A_4^* (S_5) corresponds to promotion of an electron from the HOMO to LUMO^{+2} χ_{-1}^{+2} (Fig. 2), similar to the strongly allowed S_3 state ($f=0.62$) of the planar conformation. TICT A_4^* (S_7) becomes the lowest excited state already when the polarity of the solvent reaches that of diethyl ether (Table 1 and Fig. 3), which is due to the higher dipole moment than for TICT state A_4^* (S_5). In fact, the TICT state A_4^* (S_5) corresponds to a charge transfer from the *p-N,N*-dimethylaminostyrene to the trifluoromethylsulfonylphenyl groups, centred on the phenyl ring, as presented in Fig. 2, whereas the TICT A_4^* (S_7) is due to a charge transfer from the *p-N,N*-dimethylaminostyrene to the trifluoromethylsulfonylphenyl groups, centred on the $-SO_2$ group (Fig. 2) and accordingly with a larger charge transfer distance.

For PFSDS-O23 (Table 2), the TICT states are now A_4^* (S_7) and A_4^* (S_5). In more polar solvents than Et_2O–tetrahydrofuran (THF), the TICT state A_4^* (S_7) (main character χ_{-1}^{+1}, as E^* (S_4)) becomes the lowest. The only difference relative to PFSDS is that the TICT A_4^* (S_3) (main character χ_{-1}^{+2}, as the allowed E^* (S_3) state) stays higher in energy because of its smaller dipole moment (in acetonitrile, $E_{A_4^*}(S_3)=2.52$ eV whereas $E_{F^*(S4)}=1.35$ eV) and cannot be involved in the photophysics of the molecule.

Table 3
Same as Table 1 but for PFSDS-N34

		Planar	Twisted A_1	Twisted A_2	Twisted A_5
State S_0	E_g	0	0.30	0.02	0.27
	μ_g	12.8	10.8	12.4	12.3
State S_1	E_e	3.12	3.41	3.15	3.37
	f	0.04	0.04	0.03	0.04
	μ_e	23.9	11.5	15.2	13.1
State S_2	E_e	3.35	3.74	3.37	3.57
	f	0.0000	0.0000	0.0000	1.10^{-5}
	μ_e	11.8	9.9	26.1	31.1
State S_3	E_e	3.61	3.94	3.93	3.90
	f	0.49	0.17	0.008	0.57
	μ_e	30.9	38.2	31.5	22.7
State S_4	E_e	3.74	4.15	4.11	3.98
	f	0.07	0.38	6.10^{-3}	0.004
	μ_e	36.2	22.6	12.1	37.8
State S_5	E_e	4.10	4.45	4.25	4.36
	f	8.10^{-5}	0.003	0.24	9.10^{-4}
	μ_e	10.7	20.6	19.9	17.7
State S_n	E_e		7.15 (S_{29})	4.88 (S_{10})	6.74 (S_{27})
	f		1.10^{-3}	3.10^{-3}	3.10^{-3}
	μ_e		65.4	42.9	52.1
State S_n·	E_e			5.51 (S_{18})	
	f			0.001	
	μ_e			59.4	

Conformations	States	Gas phase	n-hexane	Et_2O	THF	CH_3CN
Planar	S_1	3.12	2.91	2.73	2.66	2.58
	S_2	3.35	3.36	3.37	3.38	3.38
	S_3	3.61	3.21	2.86	2.73	2.57
	S_4	3.74	3.16	2.65	2.46	2.23
Twisted A_1	S_{29}	7.15	5.04	3.21	2.50	1.67
Twisted A_2	S_{10}	4.88	4.02	3.28	3.00	2.66
	S_{18}	5.51	3.80	2.31	1.74	1.06
Twisted A_5	S_{27}	6.74	5.44	4.31	3.88	3.36

For PFSDS-N34 (Table 3) when the solvent polarity reaches that of diethyl ether the TICT state A_2^* (S_{18}) becomes the lowest. This state (main character χ_{-2}^{+1} (94%), like the little allowed E^* (S_1) state ($f=0.04$)) corresponds to a charge transfer from the *N,N*-dimethylaniline to the trifluoromethylsulfonyl indole groups, with the acceptor orbital centred on the SO_2 unit and then presents small orbital coefficients at the linking C–C atoms. The TICT state A_1^* (S_{29}), which could be involved in the photophysics of PFSDS-N34 in acetonitrile, corresponds to a charge transfer from the dimethylamino group to the 2-phenyl-5-trifluoromethyl-sulfonyl indole, centred in the $-SO_2$ group ($HOMO^{-5} \rightarrow LUMO$ transition at 91%), presents also very small orbital coefficients at the linking C–C atoms and possesses an extremely large dipole moment (65 D).

To summarize, the quantum-chemical calculations lead to the following results relevant to the electronic spectroscopy.

(i) For PFSDS-O23, a TICT state A_4^* (S_7) is the lowest only for solvents more polar than THF whereas for PFSDS-N34, the TICT state A_2^* (S_{18}) is lower than the E^* (S_4) state even in diethyl ether (Fig. 3), because of a lower dipole moment of the planar conformation (μ_e^{E*} (S_4) = 36.2 D) compared with PFSDS-O23 (μ_e^{E*} (S_4) = 45.6 D) and a higher TICT state dipole moment (for PFSDS-N34, μ_e^{A2*} (S_{18}) = 59.4 D whereas, for PFSDS-O23, μ_e^{A4*} (S_7) = 52.6 D).

(ii) The TICT state A_5^* for the three PFSDS derivatives stays high in energy relative to the planar emitting state, even in polar solvents and is therefore probably not involved in the photophysics of these molecules.

3.2. Electronic absorption spectra

The absorption maxima of the PFSDS derivatives are reported in Table 4. A small bathochromic shift of the longest-

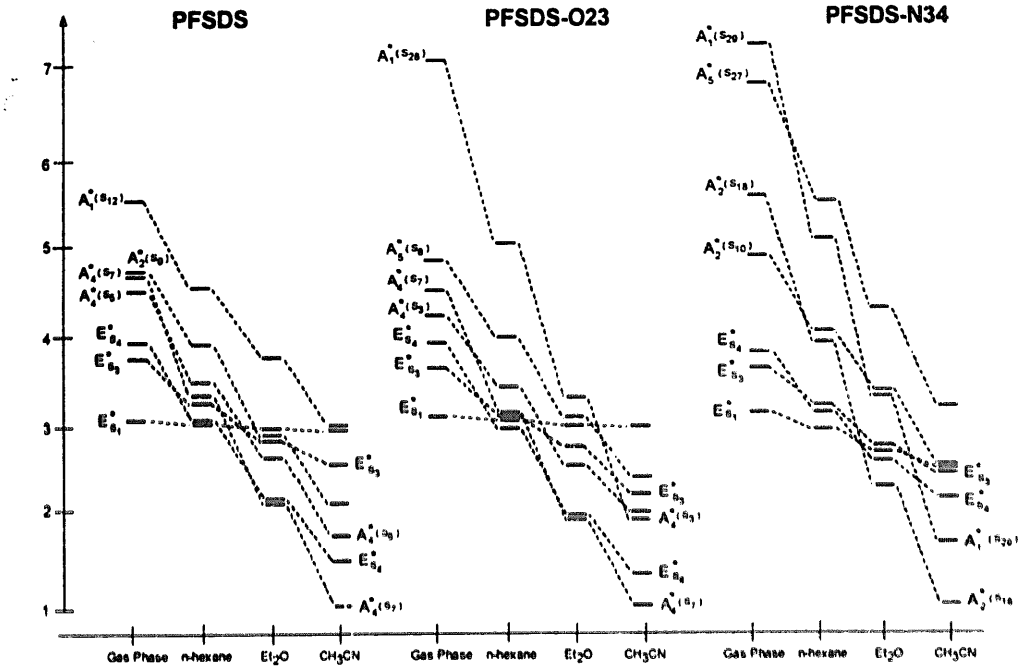

Fig. 3. Energies of the excited states for the planar conformation and lowest TICT states for differently twisted conformations of PFSDS derivatives in the gas phase, *n*-hexane ($f = 0.185$), diethyl ether (Et_2O) ($f = 0.345$) and acetonitrile (CH_3CN) ($f = 0.480$). The solvent polarity parameter used is defined in Eq. 1(a).

Table 4
Absorption maximum $\lambda^{abs}{}_{max}$ and fluorescence maxima $\lambda^{fluo}{}_{max}$, differences $\Delta\tilde{\nu}_{St}$ between the absorption and emission maxima and fluorescence quantum yields ϕ_f of PFSDS derivatives in solvents of various polarities (Δf [37]), at room temperature

Compound	Solvent	Δf	$\lambda^{abs}{}_{max}$ (nm)	$\lambda^{fluo}{}_{max}$ (nm)	$\Delta\tilde{\nu}_{St}$ (cm^{-1})	ϕ_f
PFSDS	*n*-hexane	0	402	448	2554	0.04
	Bu_2O	0.096	411	500	4331	0.09
	$CHCl_3$	0.148	416	537	5416	0.10
	Et_2O	0.167	409	518	5145	0.15
	THF	0.210	417	557	6027	0.38
	CH_2Cl_2	0.218	417	566	6313	0.14
	DMF	0.275	424	603	7001	0.27
	CH_3CN	0.305	415	593	7233	0.27
PFSDS-O23	*n*-hexane	0	407	449	2298	0.43
	Bu_2O	0.096	419	508	4181	0.49
	$CHCl_3$	0.148	423	536	4984	0.47
	Et_2O	0.167	418	529	5020	0.49
	THF	0.210	426	574	6053	0.46
	CH_2Cl_2	0.218	424	571	6072	0.32
	DMF	0.275	430	620	7127	0.08
	CH_3CN	0.305	418	611	7557	0.05
PFSDS-N34	*n*-hexane	0	365	400 421	2397	0.72
	Bu_2O	0.096	374	433	3643	0.52
	$CHCl_3$	0.148	380	459	4529	0.05
	Et_2O	0.167	376	443	4022	0.18
	THF	0.210	384	469	4720	0.04
	CH_2Cl_2	0.218	383	476	5102	0.02
	DMF	0.275	393	502	5525	0.004
	CH_3CN	0.305	384	512	6510	0.004

wavelength band can be observed for all the compounds from *n*-hexane to acetonitrile, which suggests that the Franck–Condon electronic excitation involves a relatively small transfer of charge. Nevertheless, the PFSDS derivatives undergo an additional bathochromic shift in chloroform which could result from specific interactions (Table 4).

The absorption maximum of PFSDS-N34 ($\lambda_{abs}{}^{max} = 384$ nm) is blue shifted by about 31 nm in acetonitrile, compared with PFSDS ($\lambda_{abs}{}^{max} = 415$ nm). A similar behavior is exhibited for the corresponding bridged derivative of DCS (in CH_3CN, $\lambda_{abs}{}^{max}$(DCS) = 383 nm [16] and $\lambda_{abs}{}^{max}$(DCS-N34) = 359 nm) and can be attributed to a decrease in the conjugation of the amino group with the aromatic π system, because of the (donor) nitrogen in the five-membered ring near the acceptor part. Contrary to this result, insertion of oxygen in the five-membered ring, close to the donor unit, induces no relevant change in the position of the absorption maxima between PFSDS (415 nm) and PFSDS-O23 (418 nm) or between DS (351 nm [1]) and DS-O23 (348 nm).

3.3. Emission spectra and solvatochromism

The position $\lambda_{fluo}{}^{max}$ of the fluorescence maxima and the Stokes shift $\Delta\tilde{\nu}_{St}$ are presented in Table 4. Fig. 4 shows normalized fluorescence spectra of PFSDS, measured in solvents of different polarities. The emission maxima are sensitive to solvent polarity and as recently described for donor–acceptor stilbenes [1,14–19], the spectra are completely structureless in polar solvents. The strongest solvatochromic

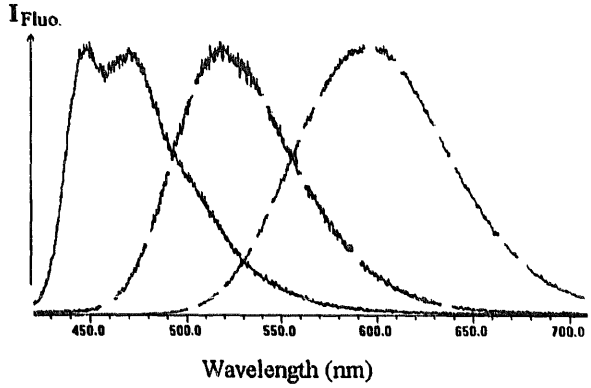

Fig. 4. Normalized fluorescence spectra of PFSDS, at room temperature, in *n*-hexane ($\Delta f = 0$) (——), diethyl ether ($\Delta f = 0.167$) (— — —) and acetonitrile ($\Delta f = 0.305$) (— — —).

Table 5
Solvatochromic slopes $m(1)$ ($cm^{-1}/\Delta f$) and $m(2)$ ($cm^{-1}/\Delta f'$) and dipole moments of various donor–acceptor stilbenes obtained according to Eqs. (4) and (5) taking into account eight solvents: *n*-hexane, Bu_2O, $CHCl_3$, Et_2O, THF, CH_2Cl_2, DMF, CH_3CN, except for DS, DCS and DCS-C34 where $CHCl_3$ was omitted. ρ is the equivalent cavity radius calculated from the molecular volumes derived from the molecular weight and the density of diphenylsulfone (1.252 g cm^{-3}) for PFSDS derivatives, benzonitrile (1.010 g cm^{-3}) for DCS derivatives and *N,N*-dimethylaniline (0.95 g cm^{-3}) for DS derivatives [26]

Compound	ρ (Å)	μ_g (D)	Slope $m(1)$	μ_e (D)	Slope $m(2)$	μ'_e (D)
DS [a]	4.53	2.41	11397	12.5	12335	11.8
DS-O23	4.62	2.41 [c]	13476	13.7		
DCS	4.60	6.95 [b]	17356	19.7		
DCS-C34	4.67	6.95 [c]	14810	19.0		
DCS-N34	4.67	6.95 [b,c]	11110	17.4		
PFSDS	6.07	6.51 [c]	15413	24.7	18540	23.5
PFSDAS	6.21	6.51 [d]	15784	25.6		
PFSDS-O23	6.11	6.51 [c,d]	17134	25.9	19864	24.6
PFSDS-N34	6.11	6.51 [c,d]	12355	23.0	17542	23.1

[a] From [1].
[b] From [38].
[c] Neglecting the effect of the five-membered ring.
[d] Calculated from the vectorial addition of the partial moment of DS and the heptafluoropropylsulfonyl group ($\mu_g = 4.1$ D, derived from the μ_g of the *p*-methoxyheptafluorosulfonylbenzene (5.4 D) with 1.3 D for the methoxy substituent of an aromatic compound [39].

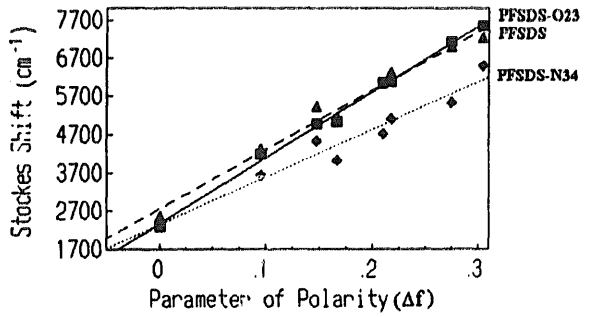

Fig. 5. Solvatochromic plot of Stokes shift for several compounds: – ▲ –, PFSDS; –■–, PFSDS-O23; – – ◆ – –, PFSDS-N34.

behavior is observed for PFSDS-O23; from *n*-hexane to acetonitrile the fluorescence spectra shifts from 449 nm to 611 nm (5900 cm^{-1}) while PFSDS-N34 shows a shift from 400 nm to 512 nm (5470 cm^{-1}). Such behavior indicates a strong difference of dipole moment between the excited state and the Franck–Condon ground state.

The difference $\Delta\mu_{eg}$ between the ground- and the excited-state dipole moments can approximately be calculated using the Lippert equation

$$\Delta\bar{\nu}_{St} = \bar{\nu}_{abs}^{max} - \bar{\nu}_{fluo}^{max} = \frac{2\,\Delta\mu_{eg}^2\,\Delta f}{hc\rho^3} + \text{constant} \qquad (4)$$

where $\Delta f = [(\epsilon-1)/(2\epsilon+1)] - [(n^2-1)/(2n^2+1)]$ represents a measure for solvent polarity, defined by the dielectric constant ϵ and the optical refractive index [37]. The slopes $m(1)$ of a plot of $\Delta\bar{\nu}_{St}$ vs. Δf for the nine compounds are collected in Table 5.

Eq. (4) assumes that the fluorescence corresponds to the Franck–Condon excited state reached directly upon excitation but, if a TICT state is the emitting state (see discussion below), according to Mataga et al. [40a] and Liptay [40b] the solvatochromic shift of the emission spectra should be used for estimating the excited-state dipole moments μ'_e:

$$\nu_{fluo}^{max} = -\frac{2\mu'_e(\mu'_e-\mu_g)\,\Delta f'}{hc\rho^3} + \text{constant} \qquad (5)$$

with $\Delta f' = [(\epsilon-1)/(2\epsilon+1)] - 0.5[(n^2-1)/(2n^2+1)]$. Considering that the resultant dipole moments μ_e and μ'_e are only approximate because of (i) the rough evaluation of ρ, which is a very important parameter for this model because the observable slopes are proportional to μ^2/ρ^3 [40] and (ii) the non-linearity of the bridged compounds, which leads to a small variation in the dipole moment direction from ground to excited states, the excited state dipole moments μ_e and μ'_e (listed in Table 5) are similar within the experimental uncertainty. Nevertheless the introduction of the nitrogen in the five-membered ring (near the acceptor part) induces a decrease $m(1)$ in the slope, as compared with the flexible molecules (Fig. 5); that is for the same substituents a lowering of the variation in the charge transfer between the ground and the excited states (DCS-N34 vs. DCS and PFSDS-N34 vs. PFSDS). Such a decrease in the excited-state dipole moment from PFSDS to PFSDS-N34 is in good agreement with the data obtained by quantum-chemical calculations (Tables 1–3), where the dipole moment of the planar conformation for PFSDS (μ_e^{E*} (S_4) = 44.7 D) is higher than for PFSDS-N34 (μ_e^{E*} (S_4) = 36.2 D).

On the contrary, the oxygen, included in the five-membered ring, in position 2,3 (i.e. near the donor part), induces a slight increase in the excited-state dipole moment (Table 5, DS-O23 vs. DS and PFSDS-O23 vs. PFSDS).

3.4. Fluorescence quantum yields

The fluorescence quantum yields ϕ_f of the three PFSDS and of the two bridged analogues without the perfluorooctyl-

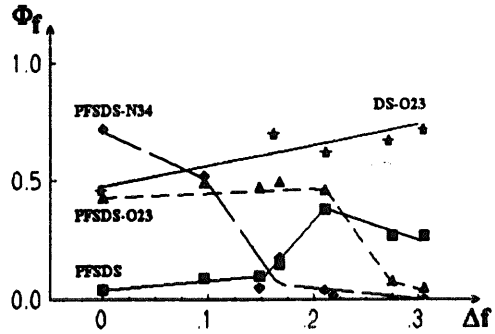

Fig. 6. Fluorescence quantum yields as a function of solvents listed in Table 5, for PFSDS (-■-), PFSDS-N34 (- ♦ -), PFSDS-O23 (- ▲ -) and DS-O23 (▲).

sulfonyl group have been measured in eight solvents (Fig. 6, Tables 4 and 6). Three groups of compounds can be considered.

(i) *Group 1*: the polar compounds with the strong acceptor group $-SO_2C_8F_{17}$ and the free double bond (PFSDS and PFSDAS) have a low fluorescence quantum yield in *n*-hexane (ϕ_f (PFSDS) = 0.04 and ϕ_f (PFSDAS) = 0.03), which increases in moderately polar solvents and decreases slightly in polar solvents.

(ii) *Group 2*: the bridged perfluorosulfonyl derivatives (PFSDS-O23 and PFSDS-N34) present a high fluorescence quantum yield in *n*-hexane (0.4–0.7), which decreases continuously with the polarity of the solvent (PFSDS-N34) or falls only when the polarity reaches that of THF (PFSDS-O23).

(iii) *Group 3*: the bridged derivatives without the perfluorooctylsulfonyl group (DS-O23 and DCS-N34) keep a high fluorescence quantum yield whatever the solvent polarity.

3.5. Time-resolved measurements

The fluorescence lifetimes at room temperature and at 77 K of the three PFSDS compounds and the two analogues without $-SO_2C_8F_{17}$ group are presented in Table 6, according to the solvent polarity. For all the systems investigated, the fluorescence decays are satisfactorily fitted by a single-exponential model.

Similarly as defined with the fluorescence quantum yields, the lifetimes will be discussed within the three groups. For group 1, at room temperature the lifetime of PFSDS increases from *n*-hexane (0.1 ns) to acetonitrile (1.1 ns) while at 77 K it keeps a comparable value (1.6–1.9 ns) whatever the solvent polarity. For group 2, a shortening of the lifetime is observed even in medium polar solvent for PFSDS-N34, whereas for PFSDS-O23 it is only for acetonitrile that the decrease is marked. The case of PFSDS-N34 in ethanol,

Table 6
Fluorescence quantum yields ϕ_f (±10%) and lifetimes τ_f (±0.1 ns) at room temperature and 77 K of PFSDS derivatives, DS-O23 and DCS-N34 recorded in various solvents; the radiative rate constant k_f ($10^9\ s^{-1}$) is calculated from ϕ_f/τ_f and the non-radiative rate constant k_{nr} ($10^7\ s^{-1}$) from $k_f(1/\phi_f - 1)$; as the lifetime at 77 K is insensitive to the solvent polarity, $\tau_f^{77\,K}$ (CH_3CN) corresponds to measurements in ethanol or *n*-butyronitrile

Solvent	Parameter	Value of parameter for following compound				
		PFSDS	PFSDS-O23	PFSDS-N34	DS-O23	DCS-N34
n-hexane	ϕ_f	0.04	0.43	0.72	0.46	0.51
	τ_f	0.1	2.1	1.3	1.4	1.0
	$\tau_f^{77\,K}$	1.6	2.0	1.3	1.9	1.2
	k_f	0.4	0.2	0.6	0.3	0.5
	k_{nr}	960	27	23	35	48
Et_2O	ϕ_f	0.15	0.49	0.18	0.70	0.78
	τ_f	0.3	3.0	0.3	2.1	1.6
	$\tau_f^{77\,K}$	1.9	2.8	1.3	1.9	1.4
	k_f	0.5	0.2	0.6	0.3	0.5
	k_{nr}	283	21	273	13	14
THF	ϕ_f	0.38	0.46	0.04	0.78	0.84
	τ_f	0.9	3.0	0.1	[c]	[c]
	$\tau_f^{77\,K}$	1.9	[c]	1.8	[c]	[c]
	k_f	0.4	0.2	0.4	[c]	[c]
	k_{nr}	65	23	960	[c]	[c]
CH_3CN	ϕ_f	0.27	0.05	0.004	0.69	0.75
	τ_f	1.1	0.3	<0.1	2.2	1.6
	$\tau_f^{77\,K}$	1.9	2.9 [a]	1.8 [a]	2.1 [a]	1.6 [d]
	k_f	0.2	0.2	0.6 [b]	0.3	0.5
	k_{nr}	54	380	15.10^3 [b]	13	17

[a] From measurements in *n*-butyronitrile.
[b] k_f is calculated from $1/\tau_f^{77\,K}$.
[c] Not measured.
[d] Measured in ethanol as solvent.

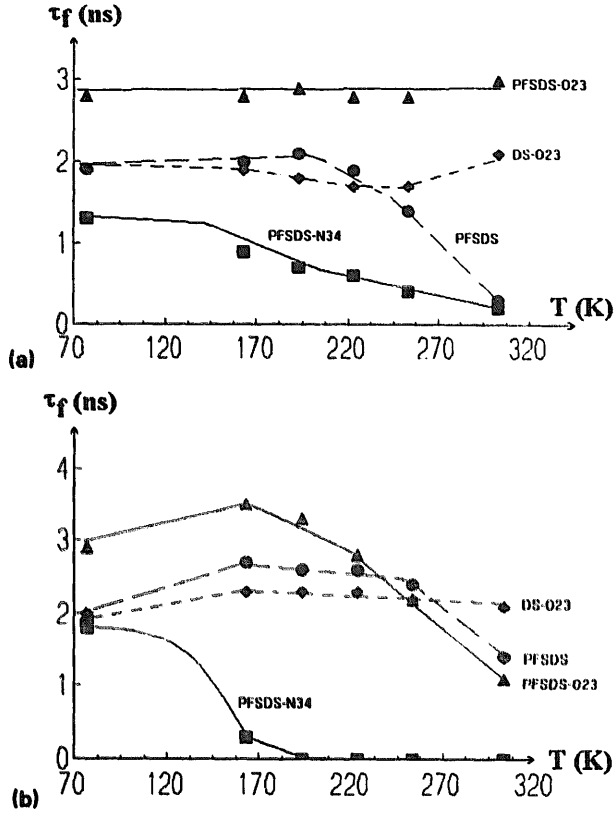

Fig. 7. Plot of the fluorescence lifetimes vs. temperature (a) in diethyl ether and (b) in *n*-butyronitrile for PFSDS (– ● –), PFSDS-N34 (–■–), PFSDS-O23 (–▲–) and DS-O23 (– ◆ –).

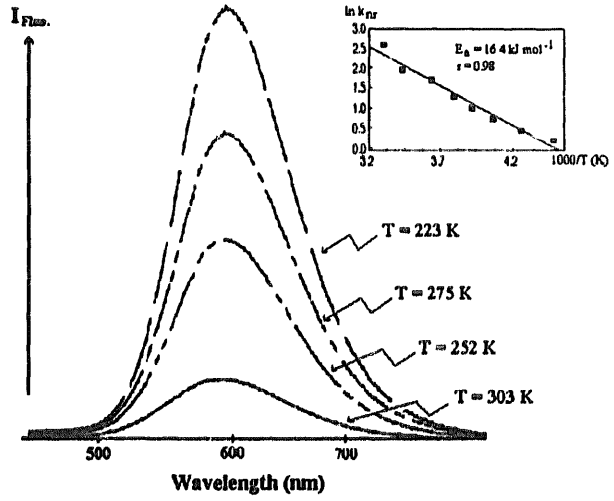

Fig. 8. Fluorescence spectra of PFSDS-O23 in ethanol vs. temperature in the range 303–223 K. The insert shows the temperature dependence $1/T$ of the logarithm k_{nr} of PFSDS-O23 in ethanol obtained from the measurement of ϕ_f, with the assumption that k_f is insensitive to the temperature as seems to be confirmed by measurements: k_f (303 K) = 0.2×10^9 s^{-1} and k_f (223 K) = 0.2×10^9 s^{-1}.

which seems to show aggregation phenomena at room temperature for a low concentration (10^{-5} mol l^{-1}), is developed in a separate paper [42]. For group 3, the lifetimes of DS-O23 and DCS-N34 are not deeply affected by the solvent polarity nor the temperature (1–1.6 ns for DCS-N34 and 1.4–2.2 ns for DS-O23).

When the temperature increases from 77 K to room temperature in butyronitrile (polar solvent) the lifetimes of fluorescence of groups 1 and 2 strongly decrease, whereas for group 3 the long lifetimes are insensitive to the temperature (Fig. 7(b)). The behavior of τ_f in diethyl ether (medium polar solvent) vs. the temperature is shown in Fig. 7(a). The same decrease in τ_f with increasing temperature is observed for compounds of group 1 and PFSDS-N34 as in polar solvents. For PFSDS-O23 and members of group 3, the long lifetimes stay unaffected by the temperature.

Table 6 gives the radiative rate k_f of fluorescence calculated from the fluorescence quantum yields ϕ_f and lifetimes τ_f at room temperature. For all the compounds investigated, the radiative rate constant is insensitive to the solvent polarity, except for PFSDS where a small decrease in k_f is observed and perhaps for PFSDS-N34, where the fluorescence lifetime at room temperature, in acetonitrile, is too short to be accurately measured (the value reported in Table 6 is that of the Franck–Condon excited state reached at 77 K which is supposed to fluoresce with a quantum yield of 1). Nevertheless the nearly identical radiative rate constants at 77 K ($1/\tau_f^{77\,K}$) and at room temperature (ϕ_f/τ_f) argue for an invariable emitting state within the solvent polarity and temperature range investigated.

The non-radiative decay rate k_{nr} data in low viscosity solvents of different polarities are also presented in Table 6. A strong decrease in k_{nr} for group 1 can be noticed as the solvent polarity is increased. In contrast, for group 2, the k_{nr} values increase with increasing solvent polarity. If we assume that the k_f value is not influenced by the temperature, the activation energy E_a for the non-radiative process (k_{nr}) can be evaluated from the measurement of ϕ_f and τ_f ($k_{nr} = k_f(1/\phi_f - 1)$) at different temperatures and the Arrhenius equation

$$k_{nr}(T) = k_{nr}^0 \exp\left(\frac{E_a}{RT}\right) \qquad (6)$$

The effect of the temperature on the fluorescence of PFSDS-O23 has been investigated from −50 °C to room temperature in diethyl ether and in ethanol. The decrease in temperature to −50 °C, in ethanol, brings about an increase in the fluorescence yield by a factor of about 6 whereas, in diethyl ether, ϕ_f is not really affected. The activation energy E_a (kJ mol^{-1}) for the non-radiative decay in ethanol is calculated (Fig. 8) to be 16.4 kJ mol^{-1}.

4. Discussion

We have recently shown that the photophysical properties of donor–acceptor stilbenes such as DCS [14–16] and DS [1,17,18] are strongly altered by the flexibility or non-flexibility of their single and double bonds (Scheme 1). In DCS, double-bond twisting leads to fluorescence quenching (state P*), whereas twisting the adjacent single bonds (bonds 2

and 4, Fig. 1) populates lower-lying emissive charge transfer states (A*, TICT [1–13]), which competes with fluorescence quenching (state P*) and therefore raises the fluorescence quantum yield and lengthens the lifetimes [16]. When by chemical bridging of the central double bond in a five-membered ring (DCS-C34 [16] and DS-C34 [14]) the state P* is not available, the quantum yield of fluorescence is only weakly affected by the solvent polarity and stays very high (about 0.8 in all the solvents investigated). However, when the acceptor group is very powerful such as a nitro group [19] or a pyridinium ion [43,44], the fluorescence quantum yield falls in polar solvents as a result of TICT state formation with non-emissive character.

The PFSDS derivatives, with the strong acceptor substituent ($-SO_2C_8F_{17}$) and the decreasing fluorescence quantum yields in polar solvents seem to belong to this last group.

For the three PFSDS derivatives in the planar conformation (E*), the state S_4 is always the lowest excited state, when the solvent is taken into account. This state corresponds to a charge transfer from the dimethylaminostilbene to the $-SO_2$ group and then presents a high dipole moment.

The TICT states A_4* (PFSDS and PFSDS-O23) and A_2* (PFSDS-N34), which involve a strong electron transfer from the donor group to the acceptor part (with the charge centred on the $-SO_2$ group), as presented for PFSDS in Fig. 3, are sufficiently stabilized to become the lowest excited states in polar solvents and to quench the fluorescence if they are non-emissive. Non-emissive properties are generally found if one of the TICT moieties possesses a small donor or acceptor system, such as the dimethylamino or nitro groups [19], whereas highly allowed charge transfer emission can arise if both moieties are large aromatic systems, as observed in biperylenyl where the TICT state is strongly vibronically coupled with the nearby excitonic state [45]. In fact, a biaryl system in the 90° twisted conformation possesses two perpendicular π systems which cannot interact if the small σ–π coupling is neglected and the TICT transition moment is zero, as well as the corresponding oscillator strength f, while the dipole moment μ_e is at a maximum [46]. However, for small deviations from 90° twisting (a more realistic representation of a TICT rotational distribution [47]) the π orbitals on the donor and acceptor start to overlap if large coefficients are present at the linking atoms. For PFSDS derivatives the non-emissive properties of the TICT states can be connected with the minimal vibronic coupling between the two aromatic systems, because of the small atomic orbital coefficient on the atoms, which link the donor and acceptor parts in the $\chi_{-1}{}^{+1}$ (PFSDS and PFSDS-O23) or $\chi_{-2}{}^{+1}$ (PFSDS-N34) transition (Fig. 2).

For PFSDS the energy of another TICT state, A_4* (S_5), is close to that of E* (S_4) even in polar solvents and therefore could participate in the fluorescence. In fact, the emissive properties of the TICT state A_4* (S_5) can be suspected (i) because of the frontier orbitals of the HOMO and LUMO² calculated, which correspond to the main transition ($\chi_{-1}{}^{+2}$, 67%), present large orbital coefficients at the linking C atoms

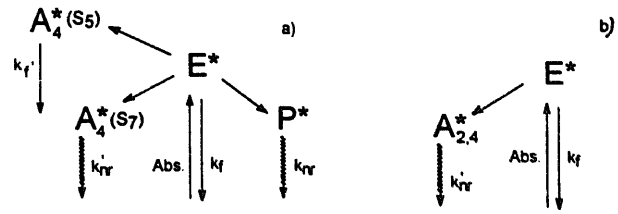

Scheme 3. (a) Four-state kinetic model proposed for the interpretation of the photophysical behavior of PFSDS, with E* (polar, emissive), P* (weakly polar, non-emissive), A_4* (S_5) (highly polar, emissive TICT state) and A_4* (S_7) (highly polar, non-emissive TICT state). (b) Two-state kinetic model used for PFSDS-O23 and PFSDS-N34.

where the donor and acceptor units decouple (Fig. 2) and (ii) because this TICT state corresponds to a similar transition as the strongly allowed S_3 state ($f = 0.62$) of the planar conformation.

The photophysical behavior of all the compounds studied can be understood using two kinetic schemes (Schemes 3(a) and 3(b)).

Compounds of group 1, represented by PFSDS, need the four-state kinetic scheme (Scheme 3(a)); the increase in ϕ_f (τ_f) from *n*-hexane to moderately polar solvents corresponds to a decrease in k_{nr} following the stabilization of the emitting state (E* (S_4) or E* (S_4) mixed with A_4* (S_5); see discussion above) more polar than the quenching state (P*). It is the general behavior occurring in donor–acceptor stilbenes [1,14–18]. In more polar solvents, there is a decrease in ϕ_f which is accounted for by the population of the non-emitting TICT state A_4* (S_7). What we cannot answer yet is why the fluorescence quantum yield of group 1 (PFSDS) is higher in polar solvents than for group 2 (PFSDS-O23), where the non-emissive state (P*) does not exist. One possible hypothesis is that the energy (1.88 eV) of the TICT state A_4* (S_5) for PFSDS (which possesses large orbital coefficients at the linking C–C atoms (Fig. 2) and therefore can be considered to be emissive), is close to that (1.53 eV) of the E* state and can be populated, whereas for PFSDS-O23 the equivalent A_4* (S_3) state has a higher energy ($E_{E^*} = 1.35$ eV and $E_{A_4^*(S_3)} = 2.52$ eV). The emissive TICT state (A_4* (S_5) for PFSDS) in polar solvent can act as a trap to the non-emissive states (P* and A_4* (S_7)) and a general increase in the fluorescence quantum yield ensues. The slight decrease in the radiative rate constant k_f of PFSDS in polar solvent is in agreement with this hypothesis, but the absence of a real difference between excited-state dipole moments estimated according to Eqs. (4) and (5) for PFSDS seem to indicate low emitting properties for the TICT state. In fact, during the solvatochromism treatment, even in polar solvents, only the charge transfer position is certainly indicated and then no difference is recorded between the hypotheses postulated in Eqs. (4) and (5).

Compounds of group 2 have their highest fluorescence quantum yield (and lifetime) already in *n*-hexane since the bridge inhibits the isomerization of the double bond and accordingly the access to the quenching state P*. Their pho-

tophysical behavior can be accounted for by a two-state kinetic scheme (Scheme 3(b)) with one emitting state (E* (S_4)) only (k_f remains constant and thus provides strong evidence against the population of an emissive TICT state, which should lead to a decrease in the k_f value [48]. Really, when the polarity of the solvent increases, the population of two non-emitting TICT states (A_2* (S_{18}) and A_1* (S_{29})) starts from *n*-hexane for PFSDS-N34 while one TICT state (A_4* (S_7)) is reached with PFSDS-O23 in THF only, because the lower energy of the E* (S_4) emitting state of PFSDS-O23 relative to that of PFSDS-N34 requires a higher solvation energy of the non-emitting TICT state (A_4* (S_7)) to be active photochemically. The formation of the non-emissive TICT state starts earlier, on the polarity scale of the solvents, for PFSDS-N34 than for PFSDS-O23, as represented by the continuous decrease in ϕ_f and increase in k_{nr} when the polarity of the solvent is increased. Such behavior is the result of two parameters, which act in the same way: (i) the dipole moment of the emissive state (E* (S_4)) is higher for PFSDS-O23 than for PFSDS-N34, as calculated using quantum-chemical calculations and measured by solvatochromism; (ii) the dipole moment of the non-emissive TICT state is larger for PFSDS-N34 than for PFSDS-O23, because of the larger distance of electron transfer between the donor (*N,N*-dimethylaniline) and the acceptor parts (2-phenyl-5-trifluoromethylsulfonyl) indole, where the charge density is localized on the $-SO_2$ group). Then from non-polar to medium polar solvents the fluorescent state is E* for PFSDS-O23, as confirmed by the long lifetime (or high quantum yield) of fluorescence and by the insensitivity of k_{nr} to the temperature (in diethylether, k_{nr} (303 K) = k_{nr} (193 K) = 21×10^7 s^{-1}). However, in polar solvents a two-state kinetic scheme is proposed for interpreting the photophysical behavior. In ethanol, when the viscosity becomes small enough for intramolecular rotation to become effective and when the temperature helps to overcome possible activation barriers, compound PFSDS-O23 efficiently reacts via the photochemical channel TICT A_4*, which shows up in the shortening of the lifetimes when the temperature increases. For PFSDS-N34, the non-radiative state is already reached in medium polar solvents (such as diethyl ether), as illustrated by the increase of the fluorescence lifetime when the temperature decreases (Fig. 7(a)).

The compounds of group 3 behave as donor–acceptor stilbenes already investigated in our previous papers [14–18]; they keep a high fluorescence quantum yield and lifetime whatever the polarity of the solvent according to a two-state kinetic scheme with a possible emitting TICT state, even if the results reported here could be accommodated by a one-state kinetic scheme (E* (S_4) state only). However, the bridging studies of DS [1,49] seem to indicate the involvement of two emissive states (E* and A_2*).

The high quantum yield and the long lifetime of fluorescence for group 3 (without the $-SO_2C_8F_{17}$ group), even in highly polar solvents, demonstrate the role of the acceptor part in the formation of non-emissive states. Contrary to the nitro derivatives [19], where the non-emissive TICT A_5* state has been shown responsible for the quenching of the fluorescence, semiempirical calculations (with our starting data as obtained by X-ray analysis of 4,4′-*N,N*-dimethylaminophenyl sulfone [50]) indicate that the energy of the TICT state involving the twisting of the $-SO_2$ group (A_5*) seems to be too high, even when solvation is introduced (Tables 1–3) and this state cannot be involved in the photophysics of PFSDS derivatives. In fact, non-emissive properties of TICT state A_5* for PFSDS derivatives, as observed for 4-nitro-4′-*N,N*-dimethylamino stilbene [19] where orbital decoupling occurs between the DS and the small NO_2 group, is not expected because the SO_2CF_3 unit can conjugate with the phenyl ring even if they are mutually perpendicular [51], owing to d hybrid orbitals of different symmetry species which are energetically available [52]. Then, in agreement with the quantum-chemical calculations, it is the A_4* TICT state, as observed with charged stilbazolium dyes [42,44], which is the better candidate for an energetically available non-emissive state or the A_2* TICT state when bond 4 is maintained planar.

5. Conclusion

The perfluorooctylsulfonyl substituent in *para* conjugation within DS derivatives leads to robust LB films and promising applications in the frequency conversion [9,10]. In this study, we have shown that a very polar Franck–Condon excited state exists (E* (S_4) in the gas phase), which is probably the emitting state S_1 in solution. Nevertheless, non-emissive TICT states become available in polar solvents which place these compounds in the same category of donor–acceptor stilbenes as the nitro [19] and the pyridinium [43,44] derivatives, characterized by a fall-off in the fluorescence intensity in polar solvents.

Acknowledgment

This work has been supported by Bundesministerium for Forschung und Technologie Project 05 414 SKT FAB9 and the EC-Large Scale Installations Program (GE 1-0018-D(B)).

References

[1] J.-F. Létard, R. Lapouyade and W. Rettig, *J. Am. Chem. Soc., 115* (1993) 2441.
[2] F.L. Carter, *Physica, 10* (1984) 175.
[3] M. Barzoukas, M. Blanchard-Desce, D. Josse, J.M. Lehn and J. Zyss, *Chem. Phys., 133* (1984) 323.
[4] J.L. Oudar, *J. Chem. Phys., 67* (1977) 446.
[5] E.M. Kosower, *Physical Organic Chemistry*, Wiley, New York, 1968.
[6] L.-T. Cheng, W. Tam, G.R. Meredith, G.L.J.A. Rikken and E.W. Meijer, *Nonlin. Opt. Prop. Org. Mater. II, 1147* (1989) 61.

[7] L.-T. Cheng, W. Tam, A. Feiring and G.L.J.A. Rikken, *Nonlin. Opt. Prop. Org. Mater. III, 1337* (1990) 203.
[8] L.-T. Cheng, W. Tam and A. Feiring, *Mol. Cryst. Lip. Cryst. Sci. Technol., Sect. B: Nonlin. Opt., 3* (1992) 69.
[9] H. Le Breton, J.-F. Létard, R. Lapouyade, A. Le Calvez, R. Maleck Rassoul, E. Freysz, A. Ducasse, C. Belin and J.-P. Morand, *Chem. Phys. Lett., 242* (1995) 604.
[10] H. Le Breton, B. Bennetau, J. Dunoguès, J.-F. Létard, R. Lapouyade, L. Vignau and J.-P. Morand, *Langmuir, 11* (1995) 1353.
[11] K. Rotkiewicz, K.H. Grellmann and Z.R. Grabowski, *Chem. Phys. Lett., 19* (1973) 315; Erratum, *Chem. Phys. Lett., 21* (1973) 212.
[12] Z.R. Grabowski, K. Rotkiewicz, A. Siemiarczuk, D.J. Cowley and W. Baumann, *Nouv. J. Chim., 3* (1979) 443.
[13] W. Rettig, in J. Mattay (ed.), *Electron Transfer I*, in *Top. Curr. Chem., 169* (1994) 253.
[14] W. Rettig and W. Majenz, *Chem. Phys. Lett., 154* (1989) 335.
[15] W. Rettig, W. Majenz, R. Lapouyade and G. Haucke, *J. Photochem. Photobiol. A: Chem., 62* (1992) 415.
[16] R. Lapouyade, K. Czeschka, W. Majenz, W. Rettig, E. Gilabert and C. Rullière, *J. Phys. Chem., 96* (1992) 9643.
[17] J.-F. Létard, R. Lapouyade and W. Rettig, *Mol. Cryst. Liq. Cryst., 236* (1993) 41.
[18] J.-F. Létard, R. Lapouyade and W. Rettig, *Chem. Phys., 186* (1994) 119.
[19] R. Lapouyade, A. Kuhn, J.-F. Létard and W. Rettig, *Chem. Phys. Lett., 208* (1993) 48.
[20] M. Vogel and W. Rettig, *Ber. Bunsenges. Phys. Chem., 91* (1987) 1241.
[21] AMPAC 5.0, ©1994, Semichem, 7128 Summit, Shawnee, KS 66216.
[22] M.J.S. Dewar, E.G. Zoebisch, E.F. Nealy and J.J.P. Stewart, *J. Am. Chem. Soc., 107* (1985) 3902.
[23] J. Del Bene and H.H. Jaffé, *J. Chem. Phys., 48* (1968) 1807, 4050; *49* (1968) 1221; *50* (1969) 1126.
[24] L.E. Sutton, *Tables of Interatomic Distances and Configuration in Molecules*, Chemical Society, London, 1965.
[25] W. Rettig and V. Bonačic-Koutecký, *Chem. Phys. Lett., 62* (1979) 115.
[26] D.R. Lide (ed.), *Handbook of Chemistry and Physics*, CRC Press, London, 73rd edn., 1992–1993.
[27] I. Furman, H.C. Geiger, D.G. Whitten, T.L. Penner and A. Ulman, *Langmuir, 10* (1994) 837.
[28] E. Haselbach and A. Schmelzer, *Helv. Chim. Acta, 54* (1971) 1299.
[29] B. Albrecht, S. Matzinger and T. Bally, *Version of MOPLOT for DOS-PCs* (available from Professor Bally, University of Fribourg, Switzerland, upon request).
[30] C.J.F. Böttcher, *Theory of Electric Polarization*, Vol. 1, Elsevier, Amsterdam, 1973.
[31] D. Majumdar, R. Sen, K. Bhattacharyya and S.P. Bhattacharyya, *J. Phys. Chem., 95* (1991) 4324.
[32] L. Onsager, *J. Am. Chem. Soc., 58* (1936) 1486.
[33] G. Orlandi and W. Siebrand, *Chem. Phys. Lett., 30* (1975) 352.
[34] L. Salem and C. Rowland, *Angew. Chem., Int. Edn. Engl., 11* (1972) 92.
[35] V. Bonačic-Koutecký, J. Koutecký and J. Michl, *Angew. Chem., Int. Edn. Engl., 26* (1987) 170.
[36] W. Rettig, W. Majenz, R. Herter, J.-F. Létard and R. Lapouyade, *Pure Appl. Chem., 65* (1993) 1699.
[37] E. Lippert, *Z. Naturforsch., 10a* (1955) 541.
[38] A. Kawski, J. Gryczyński, C.H. Jung and K.H. Heckner, *Z. Naturforsch. 32a* (1977) 420.
[39] J.W. Smith, *Electric Dipole Moments*, Butterworths, London, 1955, p. 96.
[40] (a) N. Mataga, Y. Kaifu and M. Koizumi, *Bull. Chem. Soc. Jpn., 29* (1956) 465; (b) W. Liptay, *Z. Naturforsch, 20a* (1965) 1441.
[41] W. Baumann, H. Bischof, J.-C. Fröhling, C. Brittinger, W. Rettig and K. Rotkiewicz, *J. Photochem. Photobiol. A: Chem., 64* (1992) 49.
[42] J.-F. Létard, R. Lapouyade, H. Le Breton, H. Seifert and W. Rettig, to be published.
[43] H. Ephardt and P. Fromherz, *J. Phys. Chem., 93* (1989) 7717; *95* (1991) 6792.
[44] P. Fromherz and A. Heilemann, *J. Phys. Chem., 96* (1992) 6864.
[45] J. Dobkowski, Z.R. Grabowski, B. Paeplow, W. Rettig, K.H. Koch, K. Müllen and R. Lapouyade, *New J. Chem., 18* (1994) 525.
[46] A. Klock and W. Rettig, *Pol. J. Chem., 67* (1993) 1375.
[47] M.V. Auweraer, Z.R. Grabowski and W. Rettig, *J. Phys. Chem., 95* (1991) 2083.
[48] W. Rettig, W. Majenz, R. Lapouyade and M. Vogel, *J. Photochem. Photobiol A: Chem., 65* (1992) 95.
[49] H. Seifert, W. Rettig, J.-F. Létard and R. Lapouyade, to be published.
[50] Ch. Dickinson, J.M. Stewart and H.L. Ammon, *J. Chem. Soc., Chem. Commun.*, (1970) 920.
[51] R. Rettig and E.A. Chandross, *J. Am. Chem. Soc., 107* (1985) 5617.
[52] H.P. Koch and W.E. Moffitt, *Trans. Faraday Soc., 47* (1951) 7.